Dynamics of the plasmasphere and the outer radiation belt

W. R. Johnston[1], P. C. Anderson[1], J. Goldstein[2], T. P. O'Brien[3], and S. G. Kanekal[4]

[1]W. B. Hanson Center for Space Sciences, University of Texas at Dallas, Richardson, TX [2]Space Science and Engineering Division, Southwest Research Institute, San Antonio, TX
[3]The Aerospace Corporation, Chantilly, VA [4]Laboratory for Atmospheric and Space Physics, University of Colorado at Boulder, Boulder, CO

Abstract

During geomagnetic disturbances, significant dynamics are observed in the location of the plasmapause as well as in outer radiation belt radial location and energetic particle populations. The plasmapause separates cold dense plasma in the inner magnetosphere from hot, low-density outer magnetosphere plasma, a distinction also exhibited in the characteristic plasma waves for these regions. Various wave-particle interactions inside and outside the plasmasphere are understood to be responsible for outer radiation belt particle energization and loss. We identify the plasmaspheric signature in the ionosphere—specifically the light ion trough—using DMSP spacecraft measurements. Over ten years of such observations are available from multiple DMSP satellites, coinciding with energetic particle observations by the SAMPEX spacecraft. The light ion trough is semi-automatically identified from DMSP Retarding Potential Analyzer observations of H^+ densities, then mapped along magnetic field lines to the equatorial plane. Comparisons with IMAGE EUV measurements show good agreement on plasmapause locations, with indications of plasmaspheric notches and plumes observable in the DMSP observations. The radial movement of the plasmapause location identified by DMSP during geomagnetic disturbances correlates well with the movement of the outer radiation belt zone and SAMPEX microburst observations. We are developing an extensive database of plasmapause locations, with the goal of improving understanding of the relationship between the plasmapause location and the outer radiation belt.

Plasmasphere-radiation belt interactions

The Earth's plasmasphere is dynamically influenced by magnetospheric and ionospheric electric fields. The evolution of the plasmapause during active times can significantly affect the outer radiation belt:

• *Summers et al.* (1998) argue that enhanced electromagnetic ion cyclotron (EMIC) waves within the plasmasphere tend to scatter trapped electrons into the loss cone, depleting radiation belt particles inside the plasmapause. At the same time, outside the plasmapause whistler-mode waves tend to energize trapped electrons (**Fig. 1**).

• *Goldstein et al.* (2005) found that the outer radiation belt responded to radial movement of the plasmapause during disturbed times with a time lag of several days.

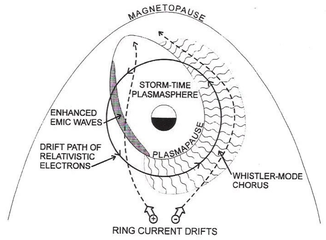

Fig. 1. Schematic of proposed mechanisms for outer radiation belt energization and loss associated with the plasmasphere. (From *Summers et al.,* 1998.)

Plasmapause-ionosphere interactions

Several ionospheric signatures of the plasmapause have been proposed, including:
- midlatitude electron density trough
- subauroral electron temp. enhancement (SETE)
- total electron content (TEC)
- light ion trough (LIT)
- precipitating electron boundary
- stable auroral red arcs (SARS)

In general, there is not a one-to-one correspondence between any of these and the plasmapause. *Taylor and Walsh* (1972) found LIT one of the more consistent signatures, whereas *Foster et al.* (1978) found the LIT generally a few degrees equatorward of the plasmapause as identified by whistler waves. *Grebowsky et al.* (1978) suggested supersonic upward H^+ flows result in LIT-plasmapause mismatch during refilling.

Satellites/instrumentation: DMSP, IMAGE, SAMPEX

DMSP: polar sun-synchronous orbits, alt. 840 km, period 100 min., generally 3-4 operational at any given time. During 2001 data is available from F12, F14, and F15 in pre-midnight to morning and F13 in dusk to dawn.

Instruments include:
- Retarding Potential Analyzer (RPA) providing ion density and composition
- Ion Drift Meter (IDM)
- Precipitating Electron and Ion Detectors (SSJ/4)

IMAGE: eccentric polar orbit (from 1400 km alt. to 8 R_E), operational 3/2000 to 12/2005. Instruments include:
- EUV imagers directly imaging 30.4 nm UV scattered by plasmaspheric He^+. Such imaging is feasible when IMAGE is near apogee (**Fig. 2**).

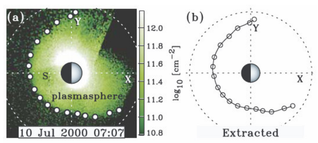

Fig. 2. Sample IMAGE EUV image of plasmasphere, showing extracted plasmapause locations. (From *Goldstein et al.,* 2004)

SAMPEX: low Earth orbit, operational 7/1992, alt. from 500 km to 620 km in 2001, includes four instruments for energetic particle measurements:
- Heavy Ion Large Area Proportional Counter Telescope (HILT)
- Low Energy Ion Composition Analyzer (LEICA)
- Mass Spectrometer Telescope (MAST)
- Proton/Electron Telescope (PET)

Method and validation

Our approach uses the DMSP-observed LIT as identification of the low-altitude plasmapause. The algorithm is illustrated in **Fig. 3**, with steps as follows (for free parameters, values used are in parenthesis):

1) DMSP H^+ density data for MLAT 20°-65° (N or S), 4-sec sampling
2) use N-point smooth (N=5)
3) reject passes where dynamic range of resulting series is less than β (β=10); also manually reject some passes (e.g. too noisy, no LIT visible on day side)
4) manually identify MLAT range around LIT density minimum
5) automatically identify minimum in smoothed density
6) proceed equatorward from minimum until density is higher than at minimum by factor f (f=1.5); this is selected as plasmapause boundary
7) compare to manually selected minimum; reject pass if this is further than Δ from PP boundary (Δ=2°)
8) (equatorward electron precipitation boundary for comparison)

Fig. 3

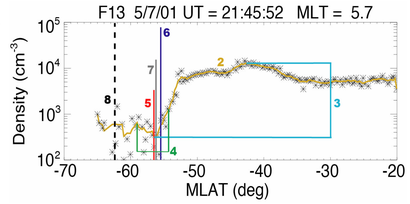

Applying this method to a 72-day period in 2001 (days 80-151), we obtained 1,790 plasmapause identifications, an average of 25 per day (range of 0 to 47 per day). This represents 12% of the DMSP passes in this period: 56% of passes were rejected automatically (step 3), 31% were rejected manually before analysis and 1% after analysis. Most identifications were from dusk to midnight or predawn to dawn.

The plasmapause locations in the ionosphere are mapped along magnetic field lines to the equatorial plasmapause, using IGRF 2000 and Tsyganenko 2001 magnetic field models.

Fig. 4 shows comparison of DMSP-identified plasmapause L values to IMAGE identifications. Points ("error" bars) show average (range) of IMAGE-extracted plasmapause locations within 15 min of time and 15 min of MLT of a DMSP identification. Comparisons form two clusters:
- Filled circles show main cluster (N=147, 79%) of good matches, with a mean L value difference of 0.45±0.43. Red line shows best fit for this cluster, blue dashed line represents identical L values.
- Open circles show second cluster of mismatches (N=40, 21%), with a mean L value difference of 1.78±0.45. Case-by-case examination of mismatches show that differences are often accounted for by highly structured plasmasphere conditions, including cases where DMSP is detecting plumes or notches.

Fig. 4

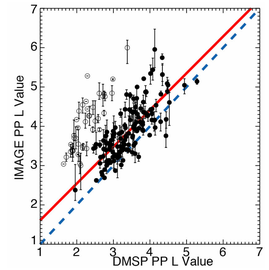

Fig. 5 illustrates one mismatch case. Left plots show DMSP H^+ observations with extracted plasmapause (red line), with three good matches and one mismatch (F15) within a 50 min. period. Right plot shows DMSP mapped orbit tracks (red lines) and DMSP plasmapause identifications (red asterisks) overlaid on an IMAGE observation projected onto the SM X-Y plane. The mismatch case maps to a plasmaspheric notch.

Fig. 5

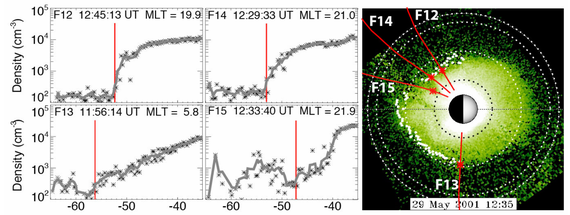

Fig. 6

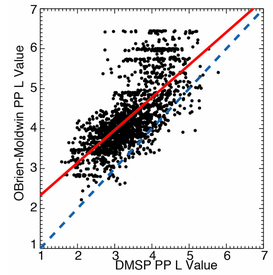

Fig. 6 shows comparison of DMSP-identified plasmapause L values to L values from plasmapause model of *O'Brien and Moldwin* (2003), parameterized by Dst and MLT. Red line shows best fit, blue line represents identical L values. Deviation for model L values greater than 5 results from model parameterization at low Dst, but could also result from problems with detection of extended plasmapause by DMSP.

Case studies: comparison to radiation belt observations

Fig. 7 shows comparisons of plasmapause location to radiation belt particle flux for three storms. Each shows SAMPEX observations of 1.5-6 MeV electron flux for L value vs. day.
- Heavy white line shows daily average plasmapause location from DMSP,
- Thin white lines show one standard deviation range in daily plasmapause location,
- Upper subplots show Dst.

Plots cover from 10 days before to 20 days after Dst peak, for storms of **(a)** 10 May 2001, Dst_{min}=-76; **(b)** 30 Oct 2003, Dst_{min}=-383; and **(c)** 20 Nov 2003, Dst_{min}=-422.

Each event shows stormtime depletion of outer radiation belt on 1-day timescale and significant erosion of plasmasphere. Afterward, outer belt is repopulated while plasmasphere refills. As plasmapause moves out into outer radiation belt, the outer belt population is depleted over a timescale of weeks.

Fig. 8 shows changes in particle flux over time following both 2003 storms: each curve shows, for a fixed L value, daily average flux of 1.5-6 MeV electrons vs. time. Diamonds indicate when the plasmapause refilled to those L values, using daily average of plasmapause identifications from DMSP. Trend is for prompt repopulation for several days, followed by longer period of depletion; change in trend is sometimes but not consistently associated with average plasmapause location.

Fig. 8

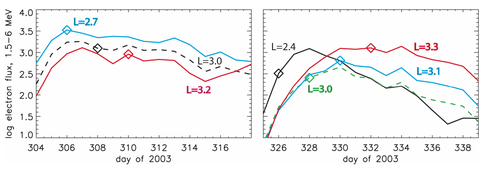

Fig. 7

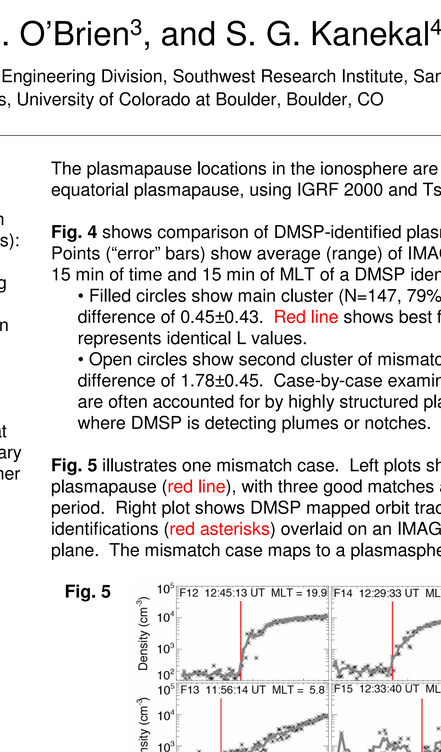

Conclusions and future work

- Comparisons of our DMSP-identified plasmapause locations to IMAGE observations show good agreement in most cases, with cases of disagreement occurring in times when the plasmasphere is highly structured. In some of these cases, indications of structure (e.g. plumes, notches) are visible in the DMSP observations.
- DMSP-identified plasmapause locations correlate with outer radiation belt dynamics for the three storm events studied. After stormtime depletion, the radiation belt is repopulated outside the plasmapause and tends to be slowly depleted when the plasmasphere refills to overlap with it. Change from repopulation to depletion does not consistently correspond to average plasmapause location, however.

We plan to make the plasmapause identification algorithm more automated, then apply it to available DMSP data, covering 10+ years (a full solar cycle), potentially yielding 100,000 identifications. The resulting database will be used for case studies and for long term statistical studies of outer radiation belt changes in relation to plasmasphere dynamics.

Acknowledgements

We gratefully acknowledge our data sources: the SAMPEX Data Center, ACE Data Center, NASA IMAGE mission, the Kyoto Data Center for Dst data, and the Center for Space Sciences at the University of Texas at Dallas and USAF for DMSP data. This work is supported by NASA NESSF grant NNX07AU71H.

References

- Foster, J. C., et al. (1978), *JGR* 83:1175-1182.
- Goldstein, J., et al. (2004), *GRL* 31:L01801.
- Goldstein, J., S. G. Kanekal, D. N. Baker, B. R. Sandel (2005), *GRL* 32:L15104.
- Grebowksy, J. M., et al. (1978), Planet. Space Sci., 26:651-660.
- O'Brien, T. P., and M. B. Moldwin (2003) *GRL* 30:1152.
- Summers, D., R. M. Thorne, F. Xiao (1998), *JGR* 103(A9):20487-20500.
- Taylor, H. A., Jr., and W. J. Walsh (1972), *JGR* 77:6716-6723.